International Journal of Fluid Power, 2014
Vol. 15, No. 3, 181–196, http://dx.doi.org/10.1080/14399776.2014.981134

Taylor & Francis
Taylor & Francis Group

Robust fault diagnosis of an electro-hydrostatic actuator using the Novel dynamic second-order SVSF and IMM strategy

Hamed H. Afshari[a], Stephen Andrew Gadsden[b]* and Saeid R. Habibi[a]

[a]*Department of Mechanical Engineering, McMaster University, Hamilton, Ontario, Canada;* [b]*Department of Mechanical Engineering, University of Maryland, Baltimore County, Maryland, USA*

(*Received 31 July 2014; accepted 23 October 2014*)

This paper introduces a new robust fault detection and identification (FDI) structure applied to an electro-hydrostatic actuator (EHA) experimental setup. This FDI structure consists of the dynamic second-order smooth variable structure filter (Dynamic second-SVSF) and the interacting multiple model (IMM) strategy. The dynamic second-order smooth variable structure filter (SVSF) is a new robust-state estimation method that benefits from the robustness and chattering suppression properties of second-order sliding mode systems. It produces robust-state estimation by preserving the first and second-order sliding conditions such that the measurement error and its first difference are pushed towards zero. Moreover, the EHA prototype works under two different operational regimes that are the normal EHA mode and the faulty EHA mode. The faulty EHA setup contains two types of faults, namely friction and internal leakage. The FDI structure contains a bank of dynamic second-order SVSFs estimating state variables based on these models. The IMM strategy combines these filters in parallel and determines the particular operating regime based on the system models and the input-output data. Experimental results demonstrate superior performance in terms of accuracy, robustness, and smoothness of state estimates.

Keywords: Smooth variable structure filter; dynamic sliding mode systems; interacting multiple model; fault detection and diagnosis; hydrostatic actuator

1. Introduction

Due to the need for continuously improved operating performance, as well as improved safety and reliability, fault diagnosis systems are growing in popularity. Fault detection and identification (FDI) may be considered a subfield of control systems engineering, and concerns itself with monitoring a system's health condition, identifying the time of fault occurrence, and pinpointing the type of fault and its location. A fault is an abnormal condition or defect at the component, equipment, or sub-system level which leads to deviation of the system from its normal mode of operation.

FDI tasks can be performed using both hardware redundancy and/or analytical redundancy methods. In hardware redundancy, hardware instrumentations are replicated and repeated such as computers, sensors, actuators and other instruments, and their outputs compared for consistency. Analytical redundancy is performed using analytical or functional information of the process being monitored. Analytical or functional models are obtained and various measured signals are used to estimate unmeasured quantities (Isermann 2006). Two main approaches are commonly used in analytical redundancy-based FDI, namely signal-based and model-based approaches. Both approaches require *a priori* knowledge of the dynamic process. In signal-based approaches, the *a priori* knowledge includes a large quantity of historical process data, observations, and measurements (Isermann 2006).

Signal-based techniques usually require signal-processing tools (e.g., fast Fourier transform (FFT) and wavelet analysis), statistical techniques (e.g., statistical classifiers, partial least squares (PLS), and principle component analysis (PCA), and intelligent decision-making techniques (e.g., artificial neural networks). In the model-based approaches, the *a priori* knowledge is in the form of a model of the system that describes its dynamic behavior. Model-based FDI approaches usually involve the use of observer, state estimation, and system identification techniques.

State estimation is one of the most popular techniques for an analytical redundancy FDI task. State estimation is referred to as the task of extracting numeric values of state variables form inaccurate, uncertain and noisy measurement data (Habibi 2007). The main objectives of this task are minimizing the state estimation error (residual) as well as preserving robustness against modeling uncertainties and external noise. The state estimation-based FDI approach is based on evaluating the residual or innovation that is the difference between measurements and estimated outputs at each sample time. In order to estimate the system states or outputs, it is necessary to select an estimation filter such as the KF, EKF, PF, etc., in conjunction with a mathematical model. It involves two main stages as follows (Isermann 2006):

*Corresponding author. Email: gadsden@umbc.edu

(1) Residual generation stage in which the system inputs and outputs are used to produce a mathematical model of the process, when the difference between the model process output and the measurement is referred to as the estimation residual or innovation.
(2) Decision-making stage in which the generated residuals are checked for the likelihood of faults, and a decision rule is then made to recognize if any fault has occurred. The knowledge of process normal operation is required in this stage.

It is important to note that the residual is just a quantity that represents the inconsistency between the actual process measurement and the mathematical model output and thus it may include both system noise as well as the fault signature. Hence, in order to perform a more accurate FDI task, it is necessary to filter out the noise from the residual signal. Figure 1 presents a block-diagram of the FDI task based on state estimation. As presented, there might be noise as well as faults in the system that consists of the process, actuator, and sensors. The estimation filter is designed based on the system's model and the residual that is the difference between the filter output and the real output. The decision on the fault condition is then made by comparing statistical properties of the system's residual with the one pertaining to the normal condition.

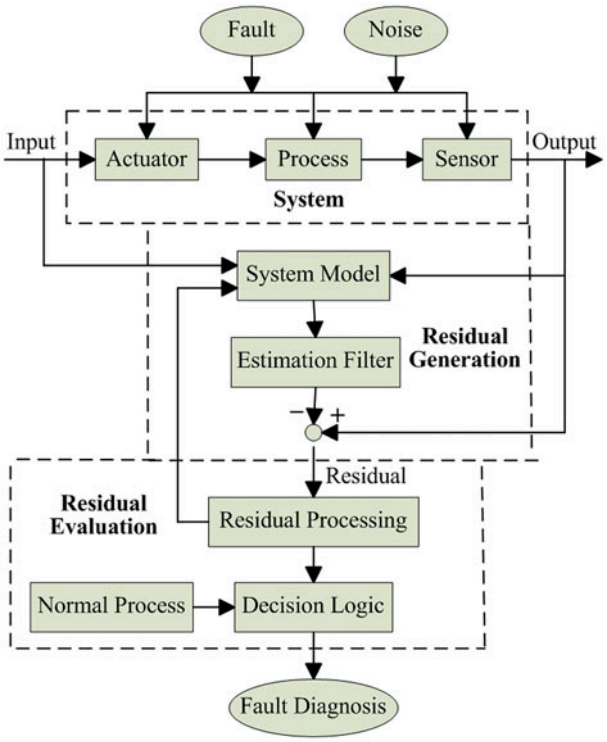

Figure 1. A block-diagram scheme of the state estimation-based FDI task.

2. An overview of state estimation

In order to estimate state variables of stochastic dynamic systems, the posterior probability density function of the state variables should be calculated using all available information. For the case with a linear state and measurement model that is subjected to Gaussian additive noise and uncertainties, it is possible to obtain an analytical solution of the *a posteriori* PDF. In such a case (e.g., Kalman filter [1960]), the *a posteriori* PDF can be expressed by only the state means and covariances. The Kalman filter (KF) has the capability to predict and update the *a posteriori* mean and covariance. For general nonlinear and non-Gaussian systems, obtaining an exact solution to this problem is impossible. However, to approximately solve nonlinear estimation problems, several techniques such as linearization and PDF approximation are required.

The extended Kalman filter (EKF) technique is the most common method for solving recursive nonlinear estimation problems based on linearization (Grewal *et al.* 2001, Bar-Shalom *et al.* 2004). The unscented Kalman filter (UKF) is an extension of the Kalman filter which utilizes an unscented transform to approximate the posterior distribution by capturing its mean and covariance accurately to the second-order. The corresponding approximation error will be in the third or higher orders (Grewal *et al.* 2001, Bar-Shalom *et al.* 2004, Ristic *et al.* 2004). It is important to note that both the EKF and the UKF are recursive minimum-mean-square-error (MMSE) estimators that approximate the posterior distribution as a Gaussian distribution. Moreover, particle filtering (PF) (Ristic *et al.* 2004) has attracted interest as a powerful tool for approximating the state *a posteriori* PDF. The PF technique uses a set of weighted particles to provide the state *a posteriori* PDF (Ristic *et al.* 2004).

Kalman-type filtering methods are primarily designed based on an exact knowledge of the system's model with known parameters. In real applications, there may be considerable uncertainties about the model structure, the physical parameters, the level of the noise, and the initial conditions. In some situations, the system dynamic is too complex to be modeled exactly, or there is no *a priori* knowledge about several parameters such as noise levels or distributions. In other situations, the system structure or parameters may change by time unpredictably. Hence, Kalman-type filtering methods may diverge or present an unacceptable performance. To overcome such potential difficulties, a robust-state estimation approach is required. The goal of a robust estimation is to construct a fixed filter that presents an acceptable performance for a wide range of modeling uncertainties.

Common robust state estimation methods found in the literature include the robust Kalman filter (the H_2 filter) (Xie *et al.* 1994, Sayed 2001, Wang and Balakrishnan 2002], the H_∞ filter (Zames 1981, Simon 2000), and the smooth variable structure filter (SVSF) (Isermann 2006, Gadsden 2011, Gadsden *et al.* 2013]. The robust Kalman

filter is designed for systems with bounded modeling uncertainties such that an upper bound of the mean square estimation error is minimized at each step (Xie *et al.* 1994). Sayed (2001) presented a general framework for robust-state estimation of dynamic systems with modeling uncertainties. Moreover, Zames (1981) introduced the main concept of the H_∞ method in the control community in 1980. This concept is later extended for the signal processing and robust-state estimation applications. The H_∞ theory is designed based on tracking the energy of a signal for the worst possible values of modeling uncertainties and measurement noise (Simon 2000). It removes the necessity of a perfect model or complete knowledge of the input statistics.

Habibi designed and implemented the new SVSF for robust-state estimation in 2007 (Habibi 2007). SVSF is a robust model-based state estimation method and formulated in a predictor-corrector form based on the sliding mode theory. Its formulation relies on a stability theorem that can result in an algorithm with an inherent switching action that guarantees convergence of state estimation to within a neighborhood of the actual states. The biggest issue with the SVSF method is chattering that is referred to as unpredictable high frequency oscillations in the state and control trajectories. It is due to the discontinuous action of the SVSF's corrective gain in a close vicinity of the real-state trajectory. However, chattering is undesirable and needs to be filtered out or at least suppressed from the state estimation trajectories. Habibi used the smoothing boundary layer in order to alleviate chattering (Habibi 2007). Note that by approximating the switching function through the smoothing boundary layer; however, the accuracy and robustness of the sliding mode system would be partially lost. Satisfying the higher order sliding conditions may be considered as an alternative to the smoothing layer that keeps the accuracy, robustness and smoothness of state estimates along with alleviating the unwanted chattering effects.

More recently, Afshari and Habibi (2013) introduced the novel second-order SVSF method as an extension to the former first-order SVSF. The second-order SVSF method applies to systems with nonlinear state model and linear measurement model. It preserves the first and second-order sliding mode conditions during state estimation. Note that satisfaction of the first and second-order sliding conditions that not only results in higher degrees of accuracy and robustness, but also decreases the amplitude of chattering and any other high frequency dynamics. The main issue with the second-order SVSF method is that it is not optimal in the mean square error sense and hence, it may be too conservative in the case with small amounts of noise and uncertainties.

The dynamic second-order SVSF (Afshari and Habibi 2014) is an advanced version of the second-order SVSF in which the second-order sliding mode condition is satisfies by defining a dynamic sliding mode manifold. This manifold is a linear combination of the sliding variable and its first time difference where the sliding variable is defined as the measurement error. It has been shown that the slope of this linear manifold represents a cut-off frequency coefficient that filters out undesirable chattering effects and is dynamically updated at each time step. The Lyapunov's second law of stability is used to prove stability of the dynamic second-order SVSF in discrete time. The Lyapunov stability criterion is defined such that it ensures reaching the dynamic sliding manifold and satisfying the first and second-order sliding conditions in finite time. Note that by proper selection of the cut-off frequency matrix, it is possible to adjust the dynamic second-order SVSF and filter out the amount of chattering that is required.

In this paper, the dynamic second-order SVSF state estimation method is initially reviewed. A novel FDI structure, which is based on the combination of the IMM strategy with the dynamic second-order SVSF, is presented and discussed in detail. This FDI structure benefits from the robustness and chattering suppression properties of the dynamic second-order SVSF; where the IMM filter is used to identify the source and type of the fault condition. The FDI structure applies to an experimental EHA setup in order to determine the current operating condition including the normal and faulty situations. The IMM strategy also determines the mode probability indicator, which represents the current operating mode of the EHA. A bank of nonlinear state models is stored in this structure and each model describes a particular operating regime. Gadsden and Song obtained these models through a series of system identification experiments (Gadsden *et al.* 2013). In order to verify the accuracy and robustness of the dynamic second-order SVSF, it is compared with other estimation methods such as the extended Kalman filter and the first-order SVSF.

3. The dynamic second-order SVSF for state estimation

The dynamic second-order SVSF (Afshari and Habibi 2014) is a model-based state estimation process that is constructed in a predictor-corrector form (similar to the well-known Kalman filter). It has two main steps including the prediction, and update steps. In the prediction step, the *a priori* state estimate $\hat{x}_{k+1|k}$ and the *a priori* state error covariance matrix $P_{k+1|k}$ are predicted using knowledge of the system prior to step k. In the update step, the predicted *a priori* state and covariance estimates are refined into the *a posteriori* state estimate $\hat{x}_{k+1|k+1}$ and covariance estimate $P_{k+1|k+1}$, respectively. The dynamic second-order SVSF applies to systems with a linear state and measurement models. In order to apply this filter to systems with nonlinear state models, the state's *a posteriori* PDF needs to be predicted using techniques involving linearization or approximation (similarly to the extended Kalman filter or the unscented Kalman filter) (Afshari and Habibi 2014).

The corrective gain of the dynamic second-order SVSF is obtained using a dynamic sliding manifold that

is defined as a linear function of the measurement error and its difference. Stability and convergence of the dynamic second-order SVSF under this manifold is proven using the Lyapunov's second law of stability. Reaching this manifold alternatively results in cancelling the measurement error and its first difference under an ideal sliding mode regime. However, due to modeling uncertainties, switching imperfections, discretization error, etc.; a real sliding regime occurs. Under the real sliding mode regime, the dynamic second-order SVSF only decreases the measurement error and its difference until reaching the existence subspace. Thereafter, it is guaranteed that they remain norm-bounded given bounded noise and modeling uncertainties.

In order to formulate the dynamic second-order SVSF, assume a stochastic dynamic system defined by a linear state and measurement models in discrete time as follows (Afshari and Habibi 2014):

$$x_k = \hat{F}x_{k-1} + \hat{G}u_{k-1} + w_{k-1}, \tag{1}$$

$$z_k = \hat{H}x_k + v_k, \tag{2}$$

where $x_k \in \mathbb{R}^{n\times 1}$ is the state vector, $u_k \in \mathbb{R}^{p\times 1}$ is the control vector, and $z_k \in \mathbb{R}^{m\times 1}$ is the measurement vector. Furthermore, $\hat{F} \in \mathbb{R}^{n\times n}$ is the estimated state matrix, $\hat{k} \in \mathbb{R}^{n\times p}$ is the estimated control matrix, $\hat{H} \in \mathbb{R}^{m\times n}$ is the estimated measurement matrix, $w_k \in \mathbb{R}^{n\times 1}$ and $v_k \in \mathbb{R}^{m\times 1}$ are the process uncertainties and measurement noise, respectively. It is also assumed that the vectors w_k and v_k are mutually independent white stochastic processes that are respectively bounded by $w_{\max}$ and $v_{\max}$ as their upper limits such that (Afshari and Habibi 2014):

$$\begin{cases} |w_{i,k}| \le w_{\max}; & i = 1,\ldots,n, \\ |v_{i,k}| \le v_{\max}; & i = 1,\ldots,m. \end{cases} \tag{3}$$

It is also assumed that they are statistically independent with respect to the state vector $x \in \mathbb{R}^{n\times 1}$. Note that in the SVSF-type filtering, the vector of sliding variables $s \in \mathbb{R}^{m\times 1}$ is defined as follows:

$$s_k = e_{z_{k|k}} = 0 \tag{4}$$

The main advantage of the dynamic second-order SVSF over other state estimation approaches is the use of a dynamic switching hyperplane that alternatively introduces an internal filtering strategy with its own cut-off frequency coefficient. In this regard, a cut-off frequency coefficient is assigned to each measurement that filters out the unwanted chattering and any other high frequency dynamics. This coefficient is formulated into the filter by defining a dynamic sliding mode formulated as follows (Afshari and Habibi 2014):

$$\sigma_k = \Delta S_k + CS_k, \tag{5}$$

where $\sigma_k : \mathbb{R}^{m\times 1} \to \mathbb{R}^{m\times 1}$ is the new sliding manifold, $S_k \in \mathbb{R}^{m\times 1}$ is the vector of sliding variables, and Δ is the backward difference operator applies on the vector of sliding variables such that: $\Delta S_k : \mathbb{R}^{m\times 1} \to \mathbb{R}^{m\times 1}$. Matrix $C = Diag(C_{it}) \in \mathbb{R}^{m\times m}$ is a diagonal matrix with entries c_{ii} representing the cut-off frequency associated to a particular measurement error $e_{z_{i,k|k}}$ (Afshari and Habibi 2014).

As a geometrical point of view, the cut-off frequency coefficient C represents the slope of the sliding manifold in a phase plane coordinated by S and ΔS. Its value affects the amount of chattering that needs to be filtered out from the state estimates. Elements of the cut-off frequency matrix C, presented in the corrective gain formulation, may be chosen by trial and error. Note that since the sliding variable and its difference are equal to the measurement error $S_k = e_{z_{k|k}}$ and its difference $\Delta S_k = e_{zk|k} - e_{z_{k-1|k-1}}$ respectively, hence by defining the sliding manifold as $\sigma_k = \Delta S_k + CS_k$ and proving the stability of state estimates about it, it is ensured that the estimation error and its difference are decreasing in finite time. After reaching the existence subspace, it is ensured that they remain norm bounded while sliding about the linear sliding manifold. Figure 2 presents the main concept of the dynamic second-order SVSF for state estimation based on the dynamic sliding manifold.

The dynamic second-order SVSF is recursively performed as follows (Afshari and Habibi 2014):

1- Prediction step [15]:

- Calculation of the *a priori* state and measurement estimates based on the system's state and measurement models as follows (Afshari and Habibi 2014):

$$\hat{x}_{k|k-1} = \hat{F}\hat{x}_{k-1|k-1} + \hat{G}u_{k-1}, \tag{6}$$

$$\hat{z}_{k|k-1} = \hat{H}\hat{x}_{k|k-1}. \tag{7}$$

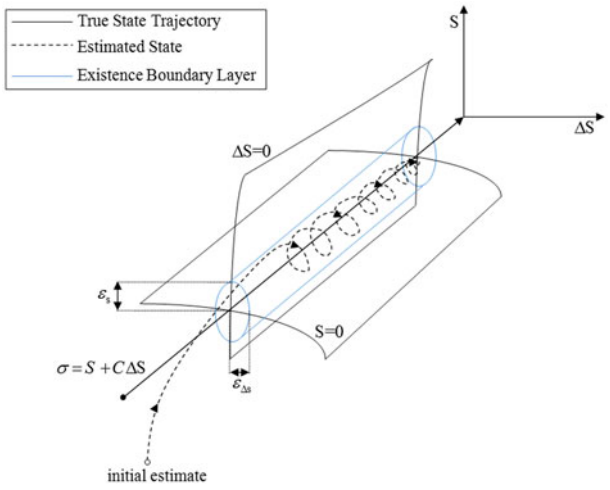

Figure 2. The dynamic second-order SVSF concept based on the dynamic sliding manifold.

- Prediction of the *a priori* state error covariance matrix as (Afshari and Habibi 2014):

$$P_{k|k-1} = \hat{F} P_{k-1|k-1} \hat{F}^T + Q_{k-1}. \tag{8}$$

- Calculation of the *a priori* and *a posteriori* measurement error vectors, $e_{z_{k|k-1}} \in \mathbb{R}^{m\times 1}$ and $e_{z_{k|k}} \in \mathbb{R}^{m\times 1}$ respectively such that (Afshari and Habibi 2014):

$$e_{z_{k|k-1}} = z_k - \hat{H}\hat{x}_{k|k-1}, \tag{9}$$

$$e_{z_{k|k}} = z_k - \hat{H}\hat{x}_{k|k}. \tag{10}$$

2-Update step [15]:

- Calculation of the innovation covariance matrix as (Afshari and Habibi 2014):

$$E_k = \hat{H} P_{k|k-1} \hat{H}^T + R_k. \tag{11}$$

- Calculation of the corrective gain for the dynamic second-order SVSF $K_k \in \mathbb{R}^{n\times 1}$ as a function of the *a priori* and the *a posteriori* measurement errors as follows (Afshari and Habibi 2014):

$$K_k = \hat{H}^{-1}\Big[e_{z_{k|k-1}} - (\gamma + \Lambda_k) e_{z_{k-1|k-1}} + \gamma \Lambda_k e_{z_{k-2|k-2}}\Big]\Big[e_{z_{k|k-1}}\Big]^{+}, \tag{12}$$

where $\Lambda_k \in \mathbb{R}^{m\times m}$ is the cut-off frequency matrix, and $\gamma = Diag(\gamma_{ii}) \in \mathbb{R}^{m\times m}$ is a diagonal matrix with positive entries such that $0 < \gamma\gamma_{ii} < 1$ represents the convergence rate pertaining to each entry. Moreover, $[]^+$ represents the pseudo-inverse operator and $\hat{H} \in \mathbb{R}^{m\times n}$ is initially assumed to be a full matrix such that all states are measurable. The dynamic second-order SVSF without full state measurement is obtained using the Luenberger observer (similar to the first-order SVSF method [Habibi 2007]).

- Update the *a priori* state estimate into the *a posteriori* state estimate $\hat{x}_{k+1|k+1}$ as (Afshari and Habibi 2014):

$$\hat{x}_{k|k} = \hat{x}_{k|k-1} + K_k e_{z_{k|k-1}}. \tag{13}$$

- Update the *a priori* state error covariance such that the *a posteriori* state error covariance $P_{k|k}$ is obtained by (Afshari and Habibi 2014):

$$P_{k|k} = (I - K_k\hat{H}) P_{k|k-1} (I - K_k\hat{H})^T + K_k R_k K_k{}^T. \tag{14}$$

Following Equation (12), the corrective gain represents a second-order Markov process and updates itself based on the measurement error values at the k and k-*1* time steps. This however leads to updating the state estimates based on information available from the last two steps ago. Having access to higher amounts of information increases the smoothness and the robustness of the dynamic second-order SVSF in comparison to first-order filters like the Kalman filter, or the first-order SVSF. Furthermore, in spite of the first-order SVSF (Habibi 2007), the dynamic second-order SVSF alleviates the unwanted chattering effect without the need for a smoothing boundary layer. Note that the smoothing layer interpolates the real discontinuities about the sliding hyperplane and hence prevents the real sliding motion that results in decreasing accuracy as well as robustness. The corrective gain formulation pushes the measurement error and its first difference towards the switching hyperplane such that the first sliding mode condition $(s_k = e_{z_{k|k}} = 0)$ and the second sliding condition $(\Delta s_k = e_{z_{k|k}} - e_{z_{k-1|k-1}} = 0)$ are satisfied under an ideal sliding mode regime. Figure 3 shows a block-diagram of the dynamic second-order SVSF for state estimation.

4. A Novel FDI structure based on the IMM filter and the dynamic Second-order SVSF

The Interacting Multiple Model (IMM) estimator is a suboptimal hybrid filter that can be combined with other state estimators. The main feature of this algorithm is the ability to estimate the state of a dynamic system with several operating modes that can switch from one mode to another. In this estimator, multiple-state equations are used to describe different operational modes of the system. A linear or nonlinear-state model is considered in order to describe each operating mode. The combination of models is used to describe the whole dynamics of the nonlinear time-varying system. A Markov transition matrix is used to calculate the probability of the system being in one of the operational modes.

Assume a hybrid linear system represents a nonlinear dynamic system in different operating modes using the state and measurement equations such that (Bar-Shalom *et al.* 2004):

$$x_{k+1} = F_{k,m_k} x_k + G_{k,m_k} u_{k,m_k} + w_{k,m_k}, \tag{15}$$

$$z_k = \hat{H}_{k,m_k} X_k + V_{k,m_k}, \tag{16}$$

The parameter m_k denotes the current system mode. Since a number of different models describes the system, the event in which the i^{th} model m_i operates may be presented by $M_{k,i} = \{m_k = m_i\}$. M denotes the set of all modes considered in the multiple models framework. It is assumed that the system model sequence is a homogenous Markov chain with transition probabilities given by (Bar-Shalom *et al.* 2004):

$$\Pr\{m_{j,k+1} | m_{i,k}\} = \pi_{ij,k}, \quad \forall i,j \in M \tag{17}$$

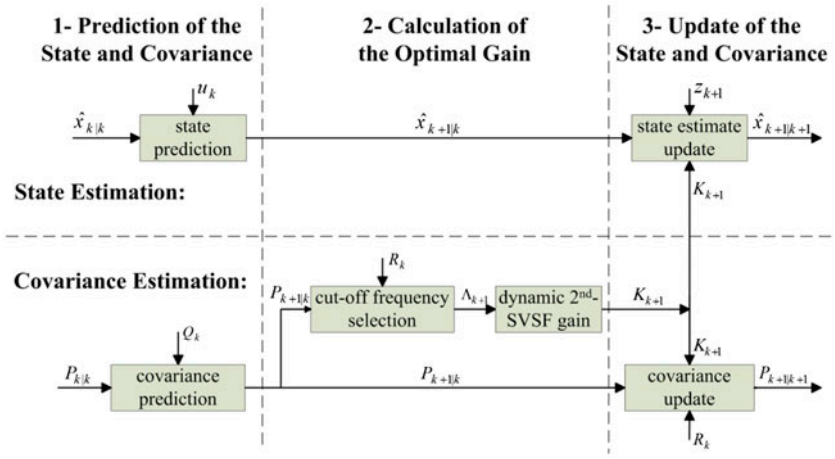

Figure 3. A block-diagram scheme of the dynamic second-order SVSF estimation process.

where π_{ij} is the Markov transition probability from mode i to mode j, when $\sum_{j=1}^{r} \pi_{ij,k} = 1$ Mode probabilities are updated at each new measurement, and weighting factors are used to calculate the state variables. One cycle of an IMM algorithm combined with the dynamic second-order SVSF consists of following three steps:

1- Interaction step

In this step, the mixing probability that is the probability of the system currently in mode i, and switching to mode j at the next step is calculated. The mixing probability, $\mu_{i|j,k-1|k-1} = \Pr\{M_{i,k-1}|M_{j,k}, Z^{k-1}\}$, is obtained as follows (Bar-Shalom *et al.* 2004):

$$\mu_{i|j,k-1|k-1} \triangleq \frac{1}{\mu_j} \pi_{ij}\, \mu_{i,k-1}, \tag{18}$$

where π_{ij} is the mode transition probability that is set by the designer. Furthermore, $\bar{\mu}_j$ is the predicted mode probability for r different modes and calculated by (Bar-Shalom *et al.* 2004):

$$\bar{\mu}_j \triangleq \Pr\{M_{j,k}|Z^{k-1}\} = \sum_{i=1}^{r} \pi_{ij}\, \mu_{i,k-1}. \tag{19}$$

The mixed initial condition is calculated using previous state and covariance estimates $\hat{x}_{i,k-1|k-1}$ and $P_{i,k-1|k-1}$, respectively. They are outputs of r different dynamic second-order SVSF filters that are based on r different operating modes. The mixed initial state and covariance matrix are calculated for the filter M_j at time k by (Bar-Shalom *et al.* 2004):

$$\hat{x}_{0j,k-1|k-1} \triangleq E\left\{x_{k-1}|M_{j,k}, Z^{k-1}\right\} = \sum_{i=1}^{r} \hat{x}_{i,k-1|k-1}\mu_{i|j}, \tag{20}$$

$$\hat{P}_{0j,k-1|k-1} = \sum_{i=1}^{r} \mu_{i|j,k-1|k-1}\left[\hat{P}_{i,k-1|k-1} + (\hat{x}_{i,k-1|k-1} - \hat{x}_{0j,k-1|k-1})(\hat{x}_{i,k-1|k-1} - \hat{x}_{0j,k-1|k-1})^T\right] \tag{21}$$

2- Filtering step

Mode-matched filtering is applied in this step and the likelihood function corresponding to each filter is determined. The calculated mixed initial state and covariance are set as inputs to the dynamic second-order SVSF which is matched to mode $M_j(k)$. The filtering step starts by predicting the state and the error covariance matrix of each mode are provided as follows (Bar-Shalom *et al.* 2004):

$$\hat{x}_{j,k|k-1} = \hat{F}_{j,k-1}\hat{x}_{0j,k-1|k-1} + \hat{G}_{j,k-1}u_{j,k-1} + \hat{w}_{j,l-1}, \tag{22}$$

$$\hat{P}_{j,k|k-1} = \hat{F}_{j,k-1}\hat{P}_{0j,k-1|k-1}\hat{F}_{j,k-1}{}^T + Q_{j,k-1}. \tag{23}$$

Similar to (8) and (10), the residual (measurement error $e_{j,k}$) and its covariance $E_{j,k}$ for each mode are respectively calculated as follows:

$$e_{j,k} = z_k - \hat{H}_{j,k}\hat{x}_{j,k|k-1}, \tag{24}$$

$$E_{j,k} = \hat{H}_{j,k}\hat{P}_{j,k|k-1}\hat{H}_{j,k}{}^T + R_{j,k}. \tag{25}$$

The dynamic second-order SVSF's gain applies for each mode such that:

$$K_{j,k} = \hat{H}_j^+[diag(e_{j,k|k-1}) - (\gamma + \Lambda_j)diag(e_{j,k|k-1}) + \gamma\Lambda_j diag(e_{j,k-2|k-2})][diag(e_{j,k|k-1})], \tag{26}$$

where $\hat{H}_j^+$ is the pseudo-inverse of the measurement matrix $\hat{H}_j$, and Λ_j is the constant cut-off frequency matrix. State and covariance updates are calculated respectively as follows:

$$\hat{x}_{j,k|k} = \hat{x}_{j,k|k-1} + K_{j,k}e_{j,k}, \tag{27}$$

$$\hat{P}_{j,k|k} = \hat{P}_{j,k|k-1} - K_{j,k}\, E_{j,k}\, K_{j,k}{}^T. \tag{28}$$

Based on the innovation matrix (residual covariance) $S_{rc_{j,k}}$, and the *a priori* measurement error $e_{j,k|k-1}$, a corresponding likelihood function $\Lambda_{j,k}$ may be calculated as follows (Bar-Shalom *et al.* 2004):

$$\Lambda_{j,k} \triangleq N[e_j, 0, E_j] = \frac{e^{-\frac{1}{2}e_{j,k}{}^T E_{j,k}{}^{-1} \upsilon e_{j,k}}}{\sqrt{2\pi E_{j,k}}}, \tag{29}$$

and the likelihood function is then used to determine the mode probability update given by (Bar-Shalom *et al.* 2004):

$$\mu_{j,k} = \frac{\bar{\mu}_j \Lambda_{j,k}}{\sum_{i=1}^{r} \bar{\mu}_i \Lambda_{i,k}}. \tag{30}$$

3- Combination step

The *a posteriori* state and covariance matrix are estimated by combining the mode conditioned estimates and covariances as (Bar-Shalom *et al.* 2004):

$$\hat{x}_{k|k} \triangleq E\left[x_k | Z^k\right] = \sum_{i=1}^{r} \hat{x}_{i,k|k} \mu_j, \tag{31}$$

$$\begin{aligned} \hat{P}_{k|k} &\triangleq E\left[\left[x_k - \hat{x}_{k|k}\right]\left[x_k - \hat{x}_{k|k}\right]^T | Z^k\right] \\ &= \sum_{j=1}^{r} P_{j,k|k} \mu_j + \sum_{i,j=1}^{r} X_{ij}, \end{aligned} \tag{32}$$

where the weighted square difference is given by (Bar-Shalom *et al.* 2004):

$$X_{ij,k} \triangleq \left[x_{i,k|k} - \hat{x}_{j,k|k}\right]\left[\hat{x}_{i,k} - \hat{x}_{j,k|k}\right]^T \mu_i \mu_j. \tag{33}$$

Figure 4 presents a block-diagram scheme of the proposed FDI structure based on the IMM filter and the dynamic second-order SVSF method.

5. Experimental electro-hydrostatic actuator (EHA) setup

The experimental setup of the electro-hydrostatic actuator (EHA) has been designed and manufactured in the Centre for Mechatronics and Hybrid Technology (CMHT) at McMaster University. This experimental setup is used to study control strategies, state and parameter estimation, and fault detection and diagnosis applications. Figure 5 presents a photo of the EHA experimental setup. The EHA uses pumping action to create pressure and move a hydraulic piston. The EHA concept is currently being used in aerospace applications and therefore its reliability and performance are highly important. Hence, health monitoring is an important element in designing EHA systems. The EHA set up includes a secondary circuit that allows a physical simulation of friction faults.

The EHA is a self-contained hydraulic system and is composed of several components including a symmetric linear actuator, a variable-speed servomotor, a bi-directional gear pump, a pressure relief valve, an accumulator, connecting tubes, and safety circuits for fault simulations. A variable-speed brushless DC electric motor, which is SIEMENS 1FK7080-5AF71-1AG2, drives the bi-directional gear pump and forces oil into the cylinder. Thereby, the gear pump can adjust the actuation performance by changing the fluid flow rate. An accumulator is used to avoid cavitation and to collect the case drain leakage from the gear pump. The pressure relief valve is used to limit the maximum system pressure to 500 psi in this case study (McCullough 2011).

The hydraulic circuit of the EHA setup has two main parts. The first part is the inner low-pressure circuit that filters the oil and preserves the minimum system pressure at 40 *psi*, by using an accumulator as well as filters and check valves. The inner circuit prevents cavitation and supplies fluid for compensating leakage. The second part of the hydraulic circuit is the outer high-pressure circuit that performs actuation. The control variable of the EHA setup is the input voltage to the motor that regulates the

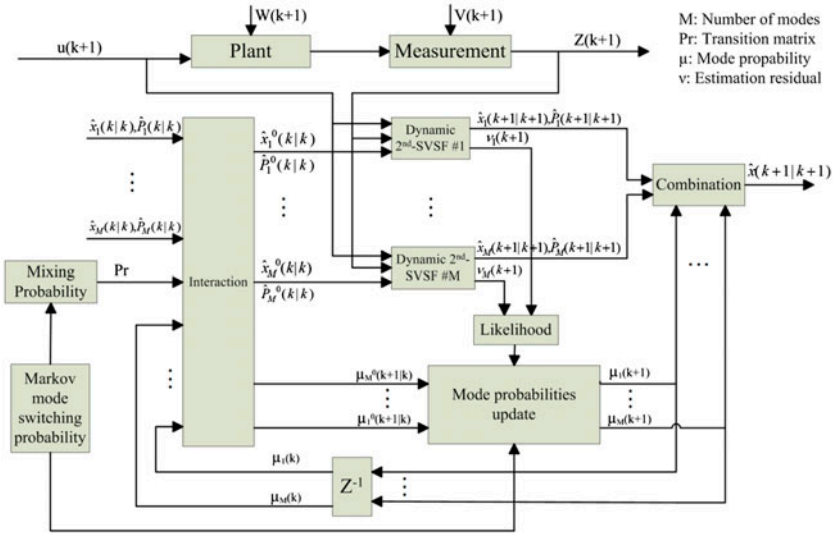

Figure 4. Block-diagram of the FDI structure as a combination of the IMM filter with the dynamic second-order SVSF.

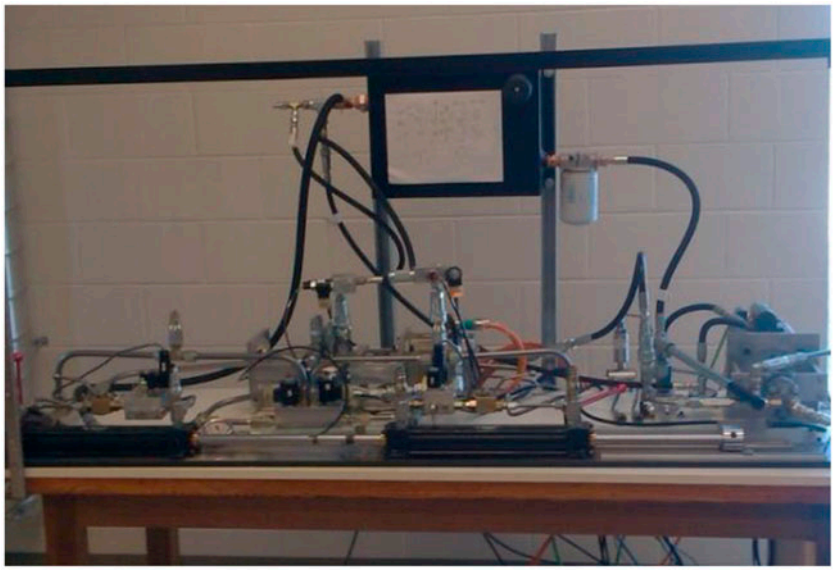

Figure 5. Experimental setup of the EHA prototype.

direction and the speed of the pump. This results in controlling the value of the fluid flow rate in the outer circuit and correspondingly adjusts the piston's position, velocity, and acceleration (McCullough 2011, Gadsden *et al.* 2013).

The circuit diagram of the EHA experimental setup is shown in Figure 6. An optical linear encoder attached to Axis A is used to obtain position measurements. Two types of fault conditions can be physically induced: internal leakage and friction. To cause or simulate a friction fault in the system, axis A in Figure 6 was used as the driving mechanism while axis B acted as a load. To implement internal leakage across the circuit, the axis A throttling valve is used (where the axis A throttle blocking valve is open). The axis A throttling valve incurs cross-port leakage between both chambers of its corresponding cylinder. Based on this fault condition, the output response of the cylinder is affected.

The EHA system is described by four state variables including the actuator position $x_1 = x$, velocity $x_2 = \dot{x}$, acceleration $x_3 = \ddot{x}$, and the differential pressure across the actuator $x_4 = P_1 - P_2$. Gadsden (Afshari and Habibi 2013) used the physical modeling approach in order to obtain the nonlinear state-space equations in discrete-time that is described as follows (Afshari and Habibi 2013):

$$x_{1,k+1} = x_{1,k} + T x_{2,k}, \tag{34}$$

$$x_{2,k+1} = x_{2,k} + T x_{3,k}, \tag{35}$$

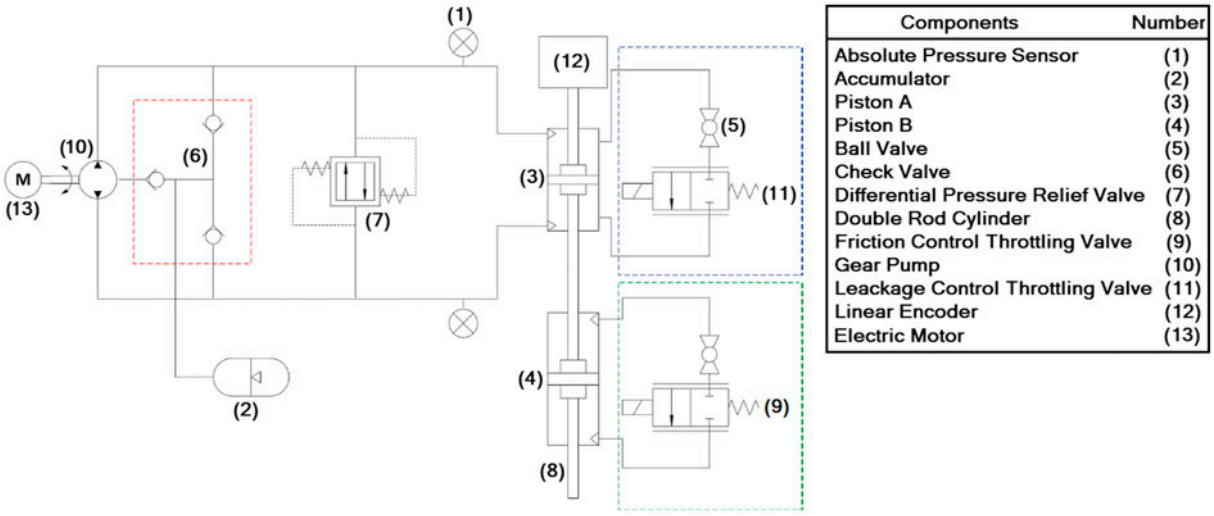

Components	Number
Absolute Pressure Sensor	(1)
Accumulator	(2)
Piston A	(3)
Piston B	(4)
Ball Valve	(5)
Check Valve	(6)
Differential Pressure Relief Valve	(7)
Double Rod Cylinder	(8)
Friction Control Throttling Valve	(9)
Gear Pump	(10)
Leackage Control Throttling Valve	(11)
Linear Encoder	(12)
Electric Motor	(13)

Figure 6. The circuit diagram of the EHA experimental setup (as per [Afshari and Habibi 2014]).

Table 1. Numeric values of the EHA parameters (Afshari and Habibi 2013).

Parameter	Physical Meaning	Parameter Values
A_E	Piston Area	1.52×10^{-3} m^2
D_p	Pump Displacement	5.57×10^{-7} m^3/rad
L	Leakage Coefficient	4.78×10^{-12} m^3/(s×Pa)
M	Load Mass	7.376 kg
Q_{L0}	Flow Rate Offset	2.41×10^{-6} m^3/s
V_0	Initial Cylinder Volume	1.08×10^{-3} m^3
β_e	Effective Bulk Modulus	2.07×10^{8} Pa

$$x_{3,k+1} = \left[1 - T\frac{a_2V_0 + M\beta_eL}{MV_0}\right]x_{3,k} - T\frac{(A_E{}^2 + a_2L)\beta_e}{MV_0}x_{2,k} + T\frac{A_E\beta_e}{MV_0} - T\frac{2a_1V_0x_{2,k}x_{3,k} + \beta_eL(a_1x_{2,k}{}^2 + a_3)}{MV_0}\text{sgn}(x_{2,k}), \tag{36}$$

$$x_{4,k+1} = \frac{a_2}{A_E}x_{2,k} + \frac{(a_1x_{2,k}{}^2 + a_3)}{A_E}\text{sgn}(x_{2,k}) + \frac{M}{A_E}x_{3,k}, \tag{37}$$

Table 2. Numeric values of the friction coefficients (Afshari and Habibi 2013).

Condition	a_1	a_2	a_3
Normal	6.589×10^{4}	2.144×10^{3}	436
Major Friction	1.162×10^{6}	-7.440×10^{3}	500
Minor Friction	4.462×10^{6}	1.863×10^{4}	551

where is T is the sample time, A_E is the piston cross-sectional area, β_e is effective bulk modulus, L is the leakage coefficient, M is the load mass, and V_0 is the initial cylinder volume. In addition, a_1, a_2, and a_3 represent the friction coefficients. Numeric values of these parameters are presented in Table 1. The input to the EHA system is also given by (Afshari and Habibi 2013):

$$u = D_p\omega_p - \text{sgn}(P_1 - P_2)Q_{L0}, \tag{38}$$

Note that D_P is the pump displacement, Q_1 is the leakage flow rate, and Q_{l0} is the parameter used to adjust offsets. It is important to notice that there are two types of parameters that are affected by the fault condition: the leakage coefficient L and the friction coefficients a_1, a_2,

Table 3. Numeric values of the leakage coefficients and flow rate offsets (Afshari and Habibi 2013).

Condition	Leakage (L)	Flow Rate Offset (Q_{L0})
Normal	4.78×10^{-12} m^3/(s×Pa)	2.41×10^{-6} m^3/s
Major Leakage	2.52×10^{-11} m^3/(s×Pa)	1.38×10^{-5} m^3/s
Minor Leakage	6.01×10^{-11} m^3/(s×Pa)	1.47×10^{-5} m^3/s

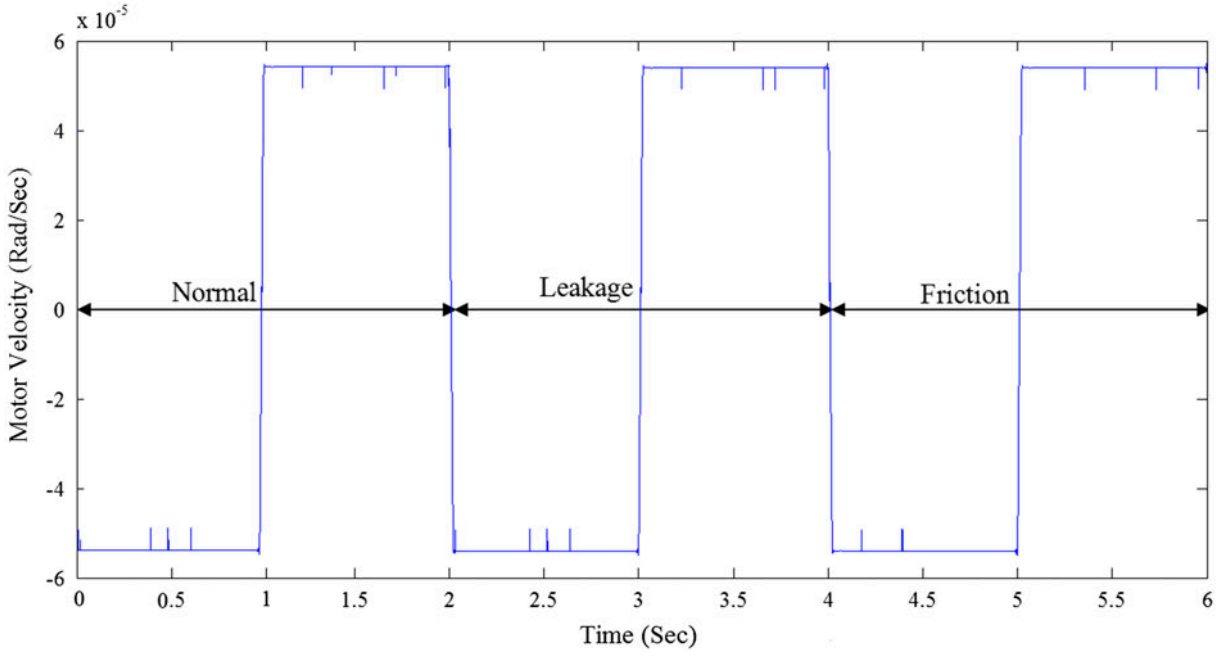

Figure 7. The input (motor's angular velocity) to the EHA experimental setup.

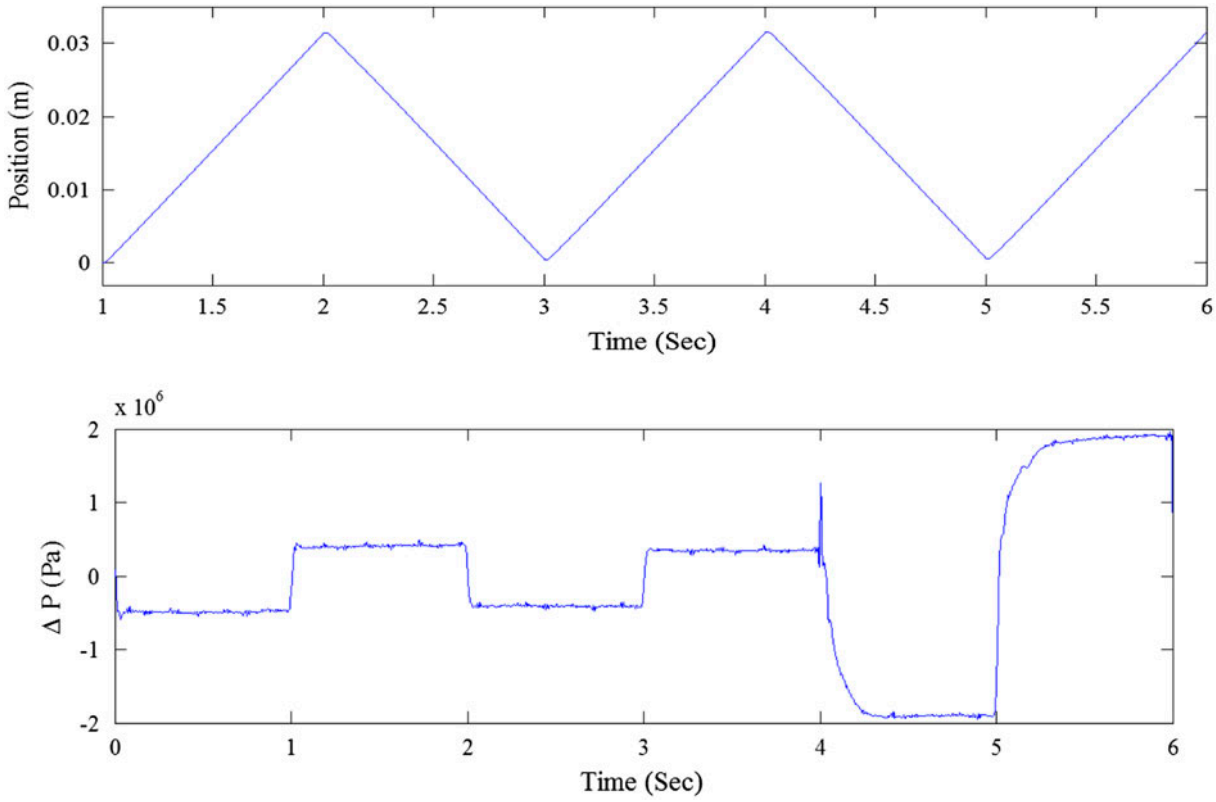

Figure 8. Profiles of the EHA outputs including the position and differential pressure.

and a_3. Hence, for accurately modeling the EHA system, numeric values of these parameters are required under different operating conditions. Table 2 lists numerical values of the friction coefficients for different operating conditions measured by experimentation as reported on (Afshari and Habibi 2013). Table 3 also presents numerical values of the leakage coefficients and flow rate offsets for these conditions (Afshari and Habibi 2013).

6. Experimental results and discussion

In this section, the FDI task is performed by combining some of the extended Kalman filter, as well as the first-order SVSF and the dynamic second-order SVSF, within an IMM structure. The EHA experimental setup is used to study and compare the IMM strategies. The software used to communicate with the EHA setup is MATLAB's Real-Time Windows Target environment. Two types of faults were physically induced to the EHA setup: internal leakage and friction. Hence, there are three main scenarios for experimentations including the normal EHA setup, the EHA with friction and the EHA with internal leakage. Each scenario applies within 2 sec separately. The sample time T for discretization is set to 0.1 ms. The cut-off frequency matrix for the dynamic second-order SVSF is set to an identity matrix. For all strategies, the initial state estimate and state error covariance matrix are defined as follows:

$$\hat{x}_{0|0} = [0 \quad 0 \quad 0]^T, \tag{39}$$

$$P_{0|0} = \begin{bmatrix} 1 & 0 & 0 \\ 0 & 10 & 0 \\ 0 & 0 & 50 \end{bmatrix}. \tag{40}$$

In order to check the dynamic second-order SVSF in terms of accuracy, and robustness of state estimates, it is compared with the extended Kalman filter (EKF), and the first-order SVSF. All of the estimation strategies are combined with the IMM filter. Several experimentations were performed with varying the pump speed to calculate the friction coefficients. Table 2 presents friction coefficients for the normal, minor leakage, and major leakage cases. Following (38), the input u to the EHA setup is a function of the motor's angular velocityω_p. The scenario that was studied involved the EHA operating normally for two seconds, a leakage fault for two seconds, followed by a friction fault for the last two seconds. The input to the EHA system is a square wave signal fluctuates between +5 and -5 rad/sec. The profile of the input is presented in Figure 7. There are four state variables including the actuator position, velocity, acceleration, and the differential pressure. The actuator position and the differential pressure are measurable, and the measurement matrix is equal to: $\hat{H} = \begin{bmatrix} 1 & 0 & 0 & 0 \\ 0 & 0 & 0 & 1 \end{bmatrix}$. Figure 8 presents profiles of the EHA outputs.

Table 4. Total RMSE values of different state estimators applied to the EHA setup.

	EKF	1st-order SVSF	Dynamic 2nd-order SVSF
$\mathbf{x_1}$	4.59×10^{-12}	1.15×10^{-12}	1.13×10^{-13}
$\mathbf{x_2}$	4.56×10^{-9}	3.91×10^{-9}	3.55×10^{-10}
$\mathbf{x_3}$	5.18×10^{-12}	6.16×10^{-14}	7.90×10^{-14}
$\mathbf{x_4}$	2.18×10^{-9}	9.64×10^{-11}	9.44×10^{-11}

Since the SVSF-type filtering needs a full measurement matrix, the Luenberger observer is used to estimate the non-measurable states (see Ref. [Afshari and Habibi 2014] for detailed information). Note that this, however, increases the amount of noise experienced by the SVSF estimation strategies. The process noise covariance Q and the measurement noise covariance R for the EKF, the first-order SVSF and the dynamic second-order SVSF methods are given by:

$$Q = Diag\left(\begin{bmatrix} 10^2 & 10^3 & 10^5 & 10^2 \end{bmatrix}\right), \tag{41}$$

$$R = Diag\left(\begin{bmatrix} 10^{-2} & 10^{-1} \end{bmatrix}\right). \tag{42}$$

The convergence rate for the first-order SVSF and the dynamic second-order SVSF are respectively set to 0.1. For the first-order SVSF, the smoothing boundary layers set to $\psi = 10 \times Diag(Q)$. For the IMM settings, the initial mode probability and the mode transition matrix are respectively set to:

$$\mu_{i,0} = \begin{bmatrix} 0.90 & 0.05 & 0.05 \end{bmatrix}^T, \tag{43}$$

$$p_{i,j} = \begin{bmatrix} 0.90 & 0.05 & 0.05 \\ 0.05 & 0.90 & 0.05 \\ 0.05 & 0.05 & 0.90 \end{bmatrix}. \tag{44}$$

It is important to note that the mode transition matrix states, for instance, that there is a 90% probability that the EHA will stay in mode 1 (normal operation) if it was in mode 1 at the current time step (i.e.,$p_{1,1} = 0.90$) (Afshari and Habibi 2013). In this study, the extended Kalman filter (EKF), the first-order SVSF and the dynamic second-order SVSF were combined with the IMM method and applied to the EHA setup for fault detection and diagnosis. Table 4 presents the root-mean-squared-error (RMSE) values of the three estimators (EKF, first-order SVSF, and the dynamic second-order SVSF when combined with the IMM filter) for the EHA with major friction. It demonstrates that under the fault condition, the IMM-based dynamic second-order SVSF provides the most accurate state estimates followed by the first-order SVSF and the EKF methods. Furthermore, Tables 5 through 7 present the mode probability estimate for each method that is called the confusion matrix. The confusion matrix represents an indication of how accurate the models are in detecting the correct operating regime.

Table 5. Confusion matrix for the IMM-EKF method (values in %).

Predicted Condition	Actual Condition	Normal	Leakage	Friction
	Normal	59.31%	27.65%	3.18%
	Leakage	40.51%	66.94%	3.53%
	Friction	0.18%	5.41%	93.29%

Table 6. Confusion matrix for the IMM-first-order SVSF method (values in %).

Predicted Condition	Actual Condition	Normal	Leakage	Friction
	Normal	91.93%	7.16%	4.07%
	Leakage	7.73%	86.41%	3.66%
	Friction	0.34%	6.43%	92.27%

Following Table 5 through Table 7, it is deduced that all of the methods successfully detected the correct operating mode (a diagonal probability of 50% or greater); however, with varying degrees of confidence. The IMM-based dynamic second-order SVSF strategy correctly identified the EHA operating normally with the highest probability level (93.33%), followed by the IMM-first order SVSF, and the IMM-EKF. The IMM-based dynamic second-order SVSF also detected the leakage fault with the highest level (90.05%), followed by the IMM-first- order SVSF, and the IMM-EKF.

Furthermore, the IMM-based EKF strategy correctly identified the friction fault with the highest confidence

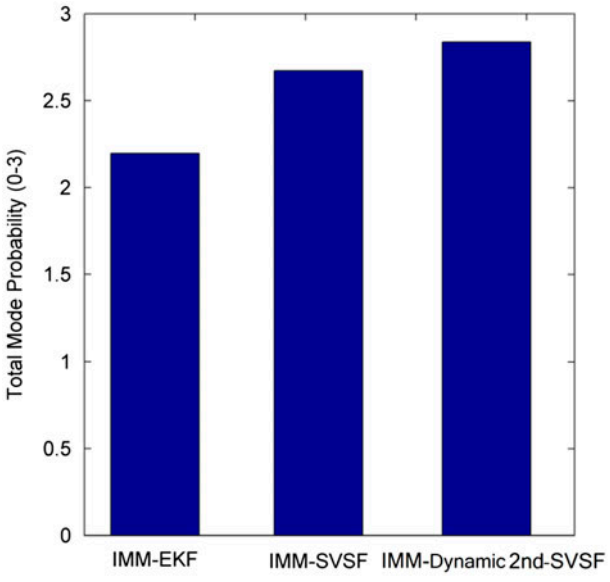

Figure 9. Total mode probability detections by different methods.

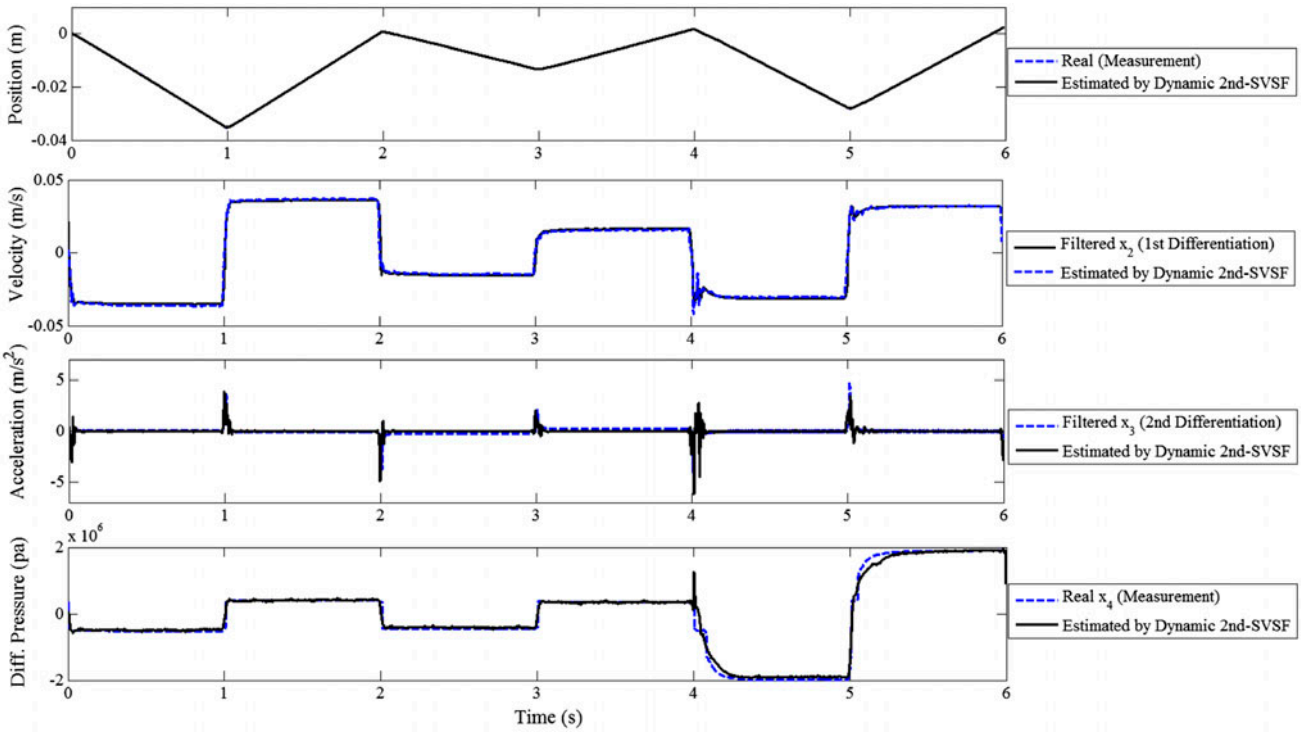

Figure 10. Profiles of the real and estimated state trajectories using the dynamic second-order SVSF.

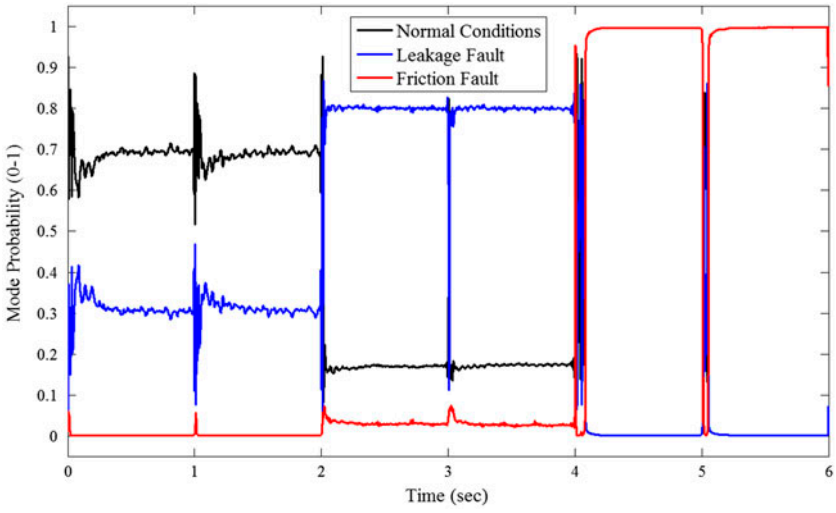

Figure 11. Mode probability of the IMM with the EKF state estimation.

level (93.29%), followed by the IMM-first-order SVSF, and the IMM-dynamic second-order SVSF. It is interesting to note that another important factor to study includes cross-detection errors or misclassifications. For example, when the EHA was operating normally, the IMM-EKF strategy detected a leakage fault with 40.51% probability. This is a high cross-detection error, as the IMM-EKF method detected normal operation with only 59.31% probability. If these values were closer, it would be difficult to properly diagnose the fault with a high level of confidence.

Another interesting factor to study is the overall correct detection probability. This can be studied by referring to the confusion matrices and Figure 9. Note that the summation of the diagonal elements in the matrices is equal to the total mode probability. Ideally, the perfect detection strategy would correctly identify the operating modes and thus, the total mode probability would be 3 or 300%. Overall, the IMM-dynamic second-order SVSF yielded the best results in terms of maximizing the correct mode detection and minimizing the misclassifications. The IMM-dynamic second-order SVSF had a total

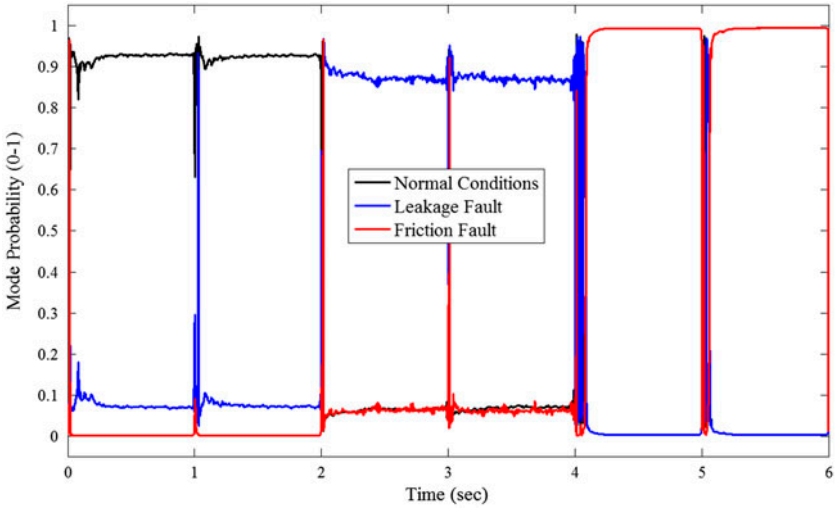

Figure 12. Mode probability of the IMM with the first-order SVSF state estimation.

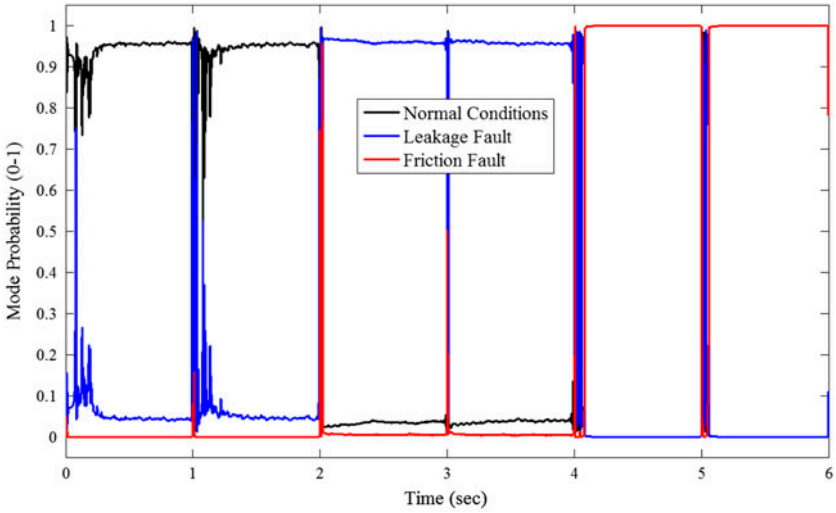

Figure 13. Mode probability of the IMM with the dynamic second-order SVSF-state estimation.

Table 7. Confusion matrix for the IMM-dynamic second-order SVSF method (values in %).

Predicted Condition	Actual Condition		
	Normal	**Leakage**	**Friction**
Normal	93.33%	4.14%	3.06%
Leakage	6.53%	90.05%	4.75%
Friction	0.14%	5.81%	92.19%

mode probability of 281.53%, followed by the IMM-first-order SVSF with a total mode probability of 270.61%, followed by the IMM-EKF with a total mode probability of 219.54%. Hence, it appears that the IMM-dynamic second-order SVSF method provides the best method for fault detection and diagnosis. This may be due to its unique gain calculation, which preserves robustness during the state estimation process.

The IMM structure with the dynamic second-order SVSF and the first-order SVSF results in estimates with larger probabilities that increases the chance of correct fault identification. This demonstrates the robust performance of the first-order and the dynamic second-order SVSF that prepare them as a powerful tool for the FDI task. Figure 10 presents the real and estimated state trajectories using the dynamic second-order SVSF method. Note that the differentiated and filtered data for the velocity and acceleration are respectively obtained by taking the first and second-order time-derivatives of the position trajectory. These signals are later filtered out through a Butterworth filter in order to remove the differentiation noise and other spikes. As demonstrated the estimated state trajectories follow the real trajectories.

Mode probability profiles of the IMM-EKF, the IMM-first SVSF and the IMM-dynamic second-SVSF strategies are respectively presented in Figures 11

Table 8. RMSE values of different state estimators combined with the IMM filter.

States	EKF	1st-order SVSF	Dynamic 2nd-order SVSF
x_1 (m)	6.59×10^{-4}	4.10×10^{-5}	1.85×10^{-5}

through 13. It is observed from these figures that the IMM-based dynamic second-order SVSF produces the largest mode probability value, followed by the IMM-based first-order SVSF, and the IMM-based EKF structures. Mode probability profiles demonstrate the superior performance of the dynamic second-order SVSF in identifying the operating mode of the EHA under the normal and uncertain conditions.

Table 8 presents the RMSE values of the four state estimators (the EKF, the first-order SVSF, and the dynamic second-order SVSF) combined with the IMM filter for the described scenario. It is deduced from Table 8 that the IMM-based dynamic second-order SVSF strategy provide the more accurate state estimates, followed by the IMM-based first-order SVSF. This however confirms the superior performance of the dynamic second-order SVSF for state estimation under the uncertain faulty situations. Numeric values of Tables 7 and 8 present the superior performance of the dynamic second-order SVSF over other estimation approaches for fault detection and diagnosis applications. Note that for a proper comparison, the inputs data as well as the initial conditions have been considered the same for all estimation methods. Furthermore, the first-order SVSF and the dynamic second-order SVSF are both tuned such that they present their best performance for state estimation under faulty conditions.

The main advantage of the dynamic second-order SVSF over other state estimation methods is its unique gain formulation that presents an adjustable internal filtering behavior within the main filtering performance. This prepares the dynamic second-order SVSF with a self-tuned cut-off frequency coefficient that determines the filter's bandwidth at each time step. Numeric value of the cut-off frequency matrix reflects the amount of chattering or any high frequency dynamics that need to be filtered out at each time step. Entries of this diagonal matrix may be selected by trial and error. Experimentations demonstrate that the dynamic second-order SVSF generates more accurate state estimates over the first-order SVSF. This is because it alleviates chattering without the need to the smoothing boundary layer that is an approximation and prevents the real sliding motion to occur. Satisfying the second-order sliding condition, instead of using the smoothing boundary layer, results in the more accurate estimates as well as simpler gain formulations. Even though the cut-off frequency coefficients need to be adjusted for each case study, however, there it removes the need for tuning the width of the boundary layer.

7. Conclusion

This paper presented a novel robust FDI strategy based on the dynamic second-order SVSF and the IMM strategy. The dynamic second-order SVSF is a robust model-based state estimation method and benefits from the robustness and chattering suppression of the second order sliding mode systems. It is able to precisely estimate state variables of the system with both nonlinear state models and linear or piece-wise linear models. The main advantage of the dynamic second-order SVSF over the first-order SVSF is improved estimation accuracy as well as its simpler structure. It removes the needs for tuning the smoothing boundary layer by trial-and-error, which saves time and design effort. The dynamic second-order SVSF is actually a trade-off between optimality and robustness. During normal operating conditions, it operates like an optimal method (e.g., Kalman filter), but for uncertain conditions, it operates as a robust state estimator.

This proposed FDI structure applies to an experimental EHA setup that operates under the normal and faulty scenarios. The faulty scenarios include the EHA setup with two major fault conditions of friction and internal leakage. The RMSE values generated by the dynamic second-order SVSF are smaller than the values of the first-order SVSF and the Kalman filter. Furthermore, the IMM-based dynamic second-order SVSF could successfully identify the correct operating regime with higher values of the mode probability. These two indices show the higher accuracy of the dynamic second-order SVSF under an experimental test that contains both the normal and faulty conditions.

List of Nomenclatures

$\mathbf{A}$	Linear state matrix
$\mathbf{A_E}$	Piston area
$\mathbf{B_E}$	Load friction
$\mathbf{C}$	Cut-off frequency coefficient
$\mathbf{D_P}$	Pump displacement
$\mathbf{E}$	Measurement error covariance
$\mathbf{F}$	Linearized state matrix
$\mathbf{G}$	Linearized control matrix
$\mathbf{H}$	Linearized measurement matrix
$\mathbf{K}$	Filter's gain
$\mathbf{L}$	Leakage coefficient
$\mathbf{M}$	Load mass
$\mathbf{P}$	State error covariance matrix
$\mathbf{Q}$	Process noise covariance matrix
$\mathbf{Q_e}$	Leakage flow rate
$\mathbf{Q_{L0}}$	Flow rate offset

$\mathbf{R}$	Measurement noise covariance matrix
$\mathbf{S}$	Vector of sliding variables
$\mathbf{T}$	Sample rate
$\mathbf{V_0}$	Initial cylinder volume
$\mathbf{a_1,a_2,a_3}$	Friction coefficients
$\mathbf{K}$	Mode number in the IMM filter
$\mathbf{M}$	Mode number in the IMM filter
$\mathbf{p_{ij}}$	Mode transition matrix
$\mathbf{S}$	Sliding mode variable
$\mathbf{V}$	Measurement noise
$\mathbf{W}$	Process noise
$\mathbf{X}$	State vector
$\mathbf{Z}$	Measurement vector
$\boldsymbol{\beta_e}$	Effective bulk modulus
$\boldsymbol{\Sigma}$	Sliding mode manifold
$\boldsymbol{\Gamma}$	Convergence rate
$\boldsymbol{\mu_i}$	Mixing probability of the i^{th} mode
$\boldsymbol{\omega_P}$	Motor rotational velocity
$\boldsymbol{\Lambda}$	Likelihood function
$\boldsymbol{\Psi}$	Smoothing boundary layer
$\mathbf{E}\{\square\}$	Expected value of an event
$\mathbf{Pr}\{\square\}$	Probability of an event
$\hat{\square}$	Estimated quantity
$\square^+$	Pseudo-inverse operator

Notes on contributors

Hamed H. Afshari is currently a Ph.D. candidate at McMaster University, and a research assistant with the Centre for Mechatronics and Hybrid Technology (CMHT). His research involves fault detection and prognostics in control systems, as well as advanced state and parameter estimation methods. Prior to joining CMHT, he obtained a M.Sc. degree in Aerospace Engineering from the University of Technology in Tehran, Iran. His research was in the area of flight dynamics and control. Hamed is a student member of the American Society of Mechanical Engineers (ASME) and the Institute of Electrical and Electronics Engineers (IEEE).

Stephen Andrew Gadsden is currently an Assistant Professor in the Department of Mechanical Engineering at the University of Maryland, Baltimore County. Andrew obtained his Ph.D. in the area of state and parameter estimation theory in 2011 from the Department of Mechanical Engineering at McMaster University, Canada. His work involved an optimal realization and further advancement of the smooth variable structure filter (SVSF). His background includes a broad consideration of state and parameter estimation strategies, the variable structure theory, fault detection and diagnosis, mechatronics, target tracking, cognitive systems, and neural networks. He is the recipient of a number of professional and scholarly awards, and was a postdoctoral Fellow with the Centre for Mechatronics and Hybrid Technology at McMaster. Andrew is an Associate Editor of the Transactions of the Canadian Society for Mechanical Engineering, and is a member of the Professional Engineers of Ontario (PEO) and the Ontario Society of Professional Engineers (OSPE). He is also a member of the American Society of Mechanical Engineers (ASME), the Institute of Electrical and Electronics Engineers (IEEE), and the Project Management Institute (PMI).

Saeid R. Habibi is currently a Professor in the Department of Mechanical Engineering at McMaster University. Saeid obtained his Ph.D. in Control Engineering from the University of Cambridge, U.K. His academic background includes research into intelligent control, state and parameter estimation, fault diagnosis and prediction, variable structure systems, and fluid power. The application areas for his research have included aerospace, automotive, water distribution, robotics, and actuation systems. He spent a number of years in industry as a Project Manager and Senior Consultant for Cambridge Control Ltd, U.K., and as Senior Manager of Systems Engineering for AlliedSignal Aerospace Canada. He received two corporate awards for his contributions to the AlliedSignal Systems Engineering Process in 1996 and 1997. He was the recipient of the Institution of Electrical Engineers (IEE) F.C. Williams best paper award in 1992 for his contribution to variable structure systems theory. He was also awarded an NSERC Canada International Postdoctoral Fellowship that he held at the University of Toronto from 1993 to 1995, and more recently a Boeing Visiting Scholar sponsorship for 2005. Saeid is on the Editorial Board of the Transactions of the Canadian Society of Mechanical Engineers and is a member of IEEE, ASME, and the ASME Fluid Power Systems Division Executive Committee.

References

Afshari, H. and Habibi, S. 2013. Second order smooth variable structure filter for parameter and state estimation. *AMSE transactions of dynamic systems, measurement and control*, DS-13–1487.

Afshari, H.H. and Habibi, S.R., Feb 2014. Optimal 2^{nd}-order smooth variable structure filter using a dynamic sliding manifold. *Automatica*.

Bar-Shalom, Y., Rong Li, X. and Kirubarajan, T., 2004. *Estimation with application to tracking and navigation*. New York: John Wiley.

Gadsden, S.A. 2011. *Smooth variable structure filtering: theory and applications*. Thesis (PhD). Mechanical Engineering Department, McMaster University, Hamilton, Canada.

Gadsden, S.A., Song, Y. and Habibi, S., 2013. Novel model-based estimators for the purpose of fault detection and diagnosis. *IEEE transactions on mechatronics*, 18 (4), 1237–1249.

Grewal, M.S. and Andrews, A.P., 2001. *Kalman filtering: theory and practice using MATLAB*. 2nd ed. New York: John Wiley.

Habibi, S., 2007. The smooth variable structure filter. *Proceedings of the IEEE*, 95, 1026–1059.

Isermann, R., 2006. *Fault diagnosis systems*. Berlin Heidelberg, Germany: Springer-Verlag.

Kalman, R.E., 1960. A new approach to linear filtering and prediction problems. *ASME transactions of basic engineering*, 82, 35–45.

McCullough, K., 2011. *Design and characterization of a dual electro-hydrostatic actuator*. Thesis (MSc). Department of Mechanical Engineering, McMaster University, Hamilton, Ontario, Canada.

Ristic, B., Arulampalam, S. and Gordon, N., 2004. *Beyond the Kalman filter: particle filters for tracking applications*. Boston: Artech House.

Sayed, A.H., 2001. A framework for state-space estimation with uncertain models. *IEEE transactions on automatic control*, 46 (7), 998–1013.

Simon, D., 2000. From here to infinity. *Embeded systems programming*, 14 (11), 20–32.

Wang, F. and Balakrishnan, V., 2002. Robust Kalman filters for linear time-varying systems with stochastic parameter uncertainties. *IEEE transactions on signal processing*, 50 (4), 803–813.

Xie, L., Soh, C. and Souza, C.E., 1994. Robust Kalman filtering for uncertain discrete-time systems. *IEEE transactions on automatic control*, 39 (6), 1310–1314.

Zames, G., 1981. Feedback and optimal sensitivity: model reference transformations, multiplicative seminorms and approximate inverses. *IEEE transactions on automatic control*, 26, 301–320.